Macromolecules
ARTICLE

Macromolecules **2010**, *43*, 8805–8812 **8805**
DOI: 10.1021/ma1018389

Surface-Initiated Living Radical Polymerization from Narrowly Size-Distributed Silica Nanoparticles of Diameters Less Than 100 nm

Kohji Ohno,*,† Tatsuki Akashi,† Yun Huang,† and Yoshinobu Tsujii†,‡

†*Institute for Chemical Research, Kyoto University, Uji, Kyoto 611-0011, Japan, and* ‡*JST, CREST, Japan*

Received August 11, 2010; Revised Manuscript Received September 21, 2010

ABSTRACT: Surface-initiated atom transfer radical polymerizations (ATRP) from narrowly size-distributed silica nanoparticles (SiNPs) of diameters less than 100 nm were investigated. Two methods were used for the preparation of the SiNP cores: one was the reverse-micelle technique, which gave monodisperse SiNPs of average diameter 55 nm, and the other was the lysine-addition technique, which gave nearly monodisperse SiNPs of average diameter 15 nm. These nanoparticles were surface-modified with a triethoxysilane derivative containing an ATRP-initiating group. The surface-initiated ATRP of methyl methacrylate (MMA) mediated by a copper complex was carried out with the initiator-fixed SiNPs in the presence of a "sacrificial" free initiator. Well-defined poly(methyl methacrylate) (PMMA) brushes of a target molecular weight were successfully grafted with a surface density as high as 0.4−0.8 chains/nm^2. These core−shell hybrid particles were highly dispersible, without any aggregation, in various solvents for PMMA. Because of the exceptionally high uniformity and perfect dispersibility, these hybrid particles formed two- and three-dimensional ordered arrays at the air−water interface and in suspension, respectively.

Introduction

Surface-initiated living radical polymerization (SI-LRP) has attracted much attention over the past decade for its excellent control of the molecular weight and polydispersity of graft polymers, and its ability to afford an exceptionally high graft density.[1−4] Thanks to the robustness and versatility of living radical polymerization (LRP),[5−10] this surface-modification technique has been applied to many types of substrates. Spherical fine particles have been surface-modified via SI-LRP in conjunction with various methods for initiator fixation, depending on the characteristics of the particle surfaces.[11−48] Silica particles (SiPs) are among the most extensively studied particles for the application of SI-LRP because of the simplicity of initiator fixation on their surfaces with organosilane compounds.[11−29,46,47] The diameters of SiPs used so far for SI-LRP range from the nanometer to the micrometer scale.

We have succeeded for the first time in preparing perfectly dispersive, monodisperse SiPs grafted with a polymer brush of high grafting density by surface-initiated atom transfer radical polymerization (SI-ATRP).[46] Thanks to the good dispersibility and high uniformity of the hybrid particles, we were able to fabricate two- or three-dimensional ordered particle arrays.[49−52] However, strategies have never been developed for the synthesis of narrowly size-distributed silica nanoparticles (SiNPs), with core diameters less than 100 nm, and having polymer brushes, which keep their perfect dispersibility in solutions. Two reasons may be given for this: one is the difficulty in obtaining narrowly size-distributed SiNPs of diameter less than 100 nm. In fact, it is difficult to prepare such nanoparticles by the Stöber method,[53] the most common method for the synthesis of monodisperse SiPs. The second reason may be that such small nanoparticles tend to form aggregates easily because of their large surface area. The aim of this work is to overcome the limitation on the size of silica particle available in this area of chemistry.

*To whom correspondence should be addressed. E-mail: ohno@scl.kyoto-u.ac.jp.

In this work, we have chosen two methods for the preparation of monodisperse SiNPs: one is the reverse-micelle-mediated technique,[54,55] in which reverse micelles act as templates for the formation of SiNPs with average diameters ranging from 30 to 70 nm. The other is the lysine-addition technique,[56−58] in which lysine controls the particle growth by adsorbing to the growing surface so as to produce nearly monodisperse SiNPs of around 10 nm in diameter. We will describe how, by preventing particle aggregation throughout all the processes from initiator fixation to polymerization, SiNPs produced by these methods are decorated by polymer brushes with high surface densities, and retain good dispersibility in solvents. We will also describe the formation of colloidal crystals using hybrid particles to demonstrate their high dispersibility and uniformity.

Experimental Section

Materials. Allyl alcohol (99%) was purchased from Wako Pure Chemicals, Osaka, Japan. 2-Bromoisobutyryl bromide (97%) and ethyl 2-bromoisobutyrate (2-(EiB)Br, 98%) were obtained from Tokyo Chemical Industry, Tokyo, Japan. 2,2′-Bipyridine (99%) was used as received from Nacalai Tesque Inc., Osaka, Japan. 4,4′-Dinonyl-2,2′-bipyridine (dNbipy, 97%) was purchased from Aldrich (St. Louis, MO, U.S.A.) and used without further purification. Copper(I) chloride (Cu^ICl, 99.9%) was purchased from Wako Pure Chemicals. Methyl methacrylate (MMA, 99%) was obtained from Nacalai Tesque Inc. and purified by flash chromatography over activated neutral alumina. A platinum catalyst (Karstedt's catalyst) solution (Pt-114, platinum content: 3 wt %) was obtained from Johnson Matthey Catalysts, Royston, U.K. Triethoxysilane (99%) and tetraethoxysilane (99.9%) were obtained from Chisso Corp., Tokyo, Japan. Igepal CO-520 was used as received from Aldrich. Ammonium hydroxide solution (28% NH_3), cyclohexane (99.5%), and *N*,*N*-dimethylformamide (DMF, 99.5%) were purchased from Wako Pure Chemicals. Water was purified by a Milli-Q system (Nihon Millipore Ltd., Tokyo, Japan) to a specific resistivity of ca. 18 MΩ cm. All other reagents were used as received from commercial sources.

Published on Web 10/05/2010

Scheme 1. Schematic Representation of the Synthesis of Fixed Initiator for Atom Transfer Radical Polymerization (ATRP), {[(2-bromo-2-methylpropionyl)oxy]propyl}triethoxysilane (BPE)

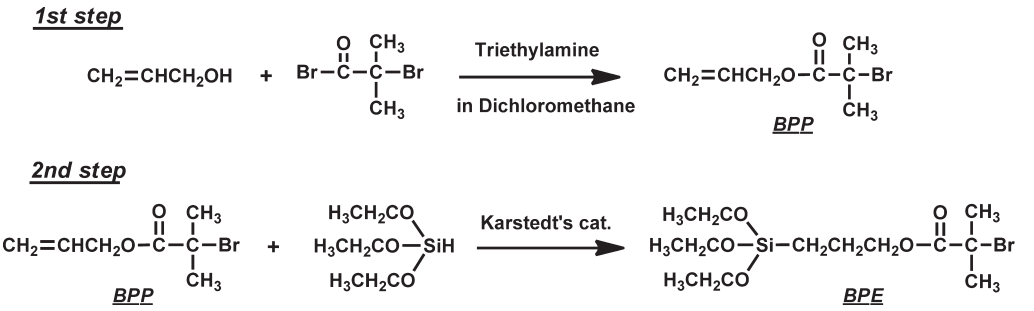

Measurements. Gel permeation chromatographic (GPC) analysis was carried out at 40 °C on a Shodex (Showa Denko K.K., Tokyo, Japan) GPC-101 high-speed liquid chromatography system equipped with a guard column (Shodex GPC KF-G), two 30 cm mixed columns (Shodex GPC KF-806 L, exclusion limit = 2×10^7), and a differential refractometer (Shodex RI-101). Tetrahydrofuran (THF) was used as the eluent at a flow rate of 0.8 mL/min. Poly(methyl methacrylate) (PMMA) standards were used to calibrate the GPC system. ^{1}H NMR (300 MHz) and ^{13}C NMR (75 MHz) spectra were obtained on a JEOL/AL300 spectrometer (JEOL, Tokyo, Japan). Elemental analyses were performed at the Laboratory of Elemental Analysis, Institute for Chemical Research, Kyoto University, Japan. The C and H contents were determined by combustion followed by differential thermal conductivity detection using a micro corder JM10 Elemental Analyzer (J-Science Lab Co., Ltd., Kyoto, Japan), and the Br contents were determined by combustion followed by ion chromatographic separation and electrical conductivity detection using a XS-100 elemental analyzer (Mitsubishi Chemical Analytech Co., Ltd., Kanagawa, Japan). Dynamic light scattering (DLS) measurements were performed in acetone solvent at 30 °C on a DLS-7000 photometer (Otsuka Electronics Co., Ltd., Osaka, Japan) with a He−Ne laser (wavelength 633 nm and power 10 mW) as a light source. The scattering light intensity was measured at a scattering angle of 90°. Data analysis was performed by the histogram method, including non-negative least-squares analysis. Transmission electron microscopy (TEM) observations were made on a JEOL transmission electron microscope (JEM-1010) operated at 100 kV. Thermal gravimetric analyses (TGA) were performed on a Shimadzu TGA-50 (Shimadzu, Kyoto, Japan) under a nitrogen atmosphere. Confocal laser scanning microscopic (CLSM) observations were made on an inverted type CLSM (LSM 5 PASCAL, Carl Zeiss, Germany) with a 488 nm wavelength Ar laser and ×63 objective (Plan Apochromat, Carl Zeiss) in reflection mode. The distance of the focal plane from the inside surface of the coverslip was 50 μm.

Synthesis of the Fixed Initiator, {[(2-Bromo-2-methylpropionyl)oxy]propyl}triethoxysilane (BPE). BPE was synthesized via a two-step reaction (Scheme 1). First step: 2-bromoisobutyryl bromide (450 g, 1.96 mol) was added dropwise to a cold solution of allyl alcohol (170 g, 2.93 mol) in dry dichloromethane (2 L) with triethylamine (238 g, 2.35 mol) at 0 °C. The mixture was magnetically stirred for 3 h at 0 °C and then for another 10 h at room temperature. The system was evaporated to dryness under reduced pressure, and the residue was diluted with THF (1 L). The system was passed through filter paper, and the filtrate was evaporated to dryness under reduced pressure. The residue was diluted with chloroform (1 L) and washed twice with 1 N HCl aqueous solution (2 × 1 L), twice with saturated $NaHCO_3$ aqueous solution (2 × 1 L), and twice with water (2 × 1 L). Drying over Na_2SO_4, filtration, and removal of the solvent gave a brown oil, which was purified by distillation under reduced pressure to yield 1-[(2-bromo-2-methylpropionyl)oxy]-2-propene (BPP) as a transparent liquid collected at ca. 1.5 mmHg and ca. 40 °C (308 g, 76%). ^{1}H NMR ($CDCl_3$): δ 1.95 (s, 6H, CCH_3), 4.68 (d, 2H, CH_2O), 5.26−5.42 (d, 2H, CH_2=CH), 5.94 (m, 1H, CH_2=CH). ^{13}C NMR ($CDCl_3$): δ 30.8 (CCH_3), 55.6 (CBr), 66.4 (CH_2O), 118.5 (CH_2=CH), 131.4 (CH_2=CH), 171.3 (C=O). Anal. Calcd for $C_7H_{11}O_2Br$: C, 40.60; H, 5.35; O, 15.45; Br, 38.59. Found: C, 40.67; H, 5.21; O, 14.65; Br, 38.38.

Second step: BPP (190 g, 918 mmol) was charged into a two-necked round-bottom flask equipped with a magnetic stirring bar and a rubber septum, and the system was deoxygenated by purging with argon. Triethoxysilane (350 g, 2.13 mol) that had been purged with argon beforehand was added into the flask in a glovebox purged with argon, and subsequently Karstedt's catalyst solution (1 g) was added to the system using a syringe. The reaction mixture was magnetically stirred under an argon atmosphere for 24 h. The complete disappearance of BPP, and hence completion of the reaction, was confirmed by ^{1}H NMR spectroscopy. (If the reaction is not complete in 24 h, it should be continued by adding a suitable amount of the catalyst to the mixture.) The system was subjected to distillation under reduced pressure to yield the initiator BPE as a transparent liquid collected at ca. 1.5 mmHg and ca. 130 °C (230 g, 67%). ^{1}H NMR ($CDCl_3$): δ 0.69 (t, 2H, $SiCH_2$), 1.23 (t, 9H, CH_3CH_2OSi), 1.80 (m, 2H, CH_2), 1.93 (s, 6H, CCH_3), 3.83 (q, 6H, CH_3CH_2OSi), 4.15 (t, 2H, CH_2O). ^{13}C NMR ($CDCl_3$): δ 6.41 ($SiCH_2$), 18.3 ($SiOCH_2CH_3$), 22.0 (CH_2), 30.8 (CCH_3), 56.0 (CBr), 58.4 ($SiOCH_2CH_3$), 68.0 (CH_2O), 171.7 (C=O). Anal. Calcd for $C_{13}H_{27}O_5BrSi$: C, 42.05; H, 7.33; Br, 21.52. Found: C, 41.78; H, 7.44; Br, 21.61.

ATRP-Initiator Fixation on SiNPs Prepared by the Reverse-Micelle-Mediated Method. SiNP cores were prepared by the reverse-micelle-mediated technique developed by Osseo-Asare et al.[54,55] In a typical run, a reverse microemulsion was prepared at room temperature by vigorously shaking a 2 L conical flask charged with a mixture of 28% NH_3 aqueous solution (4.48 g), Igepal CO-520 (27.1 g), and cyclohexane (1 L). Tetraethoxysilane (5.21 g) diluted with cyclohexane (5 mL) was added to the microemulsion, and the system was gently shaken. The mixture was allowed to stand at room temperature for 4 days. To fix the initiator onto the surface of the produced SiNPs, a mixture of BPE (5.2 g) and cyclohexane (5 mL) was added to the microemulsion system, and the system was gently shaken and allowed to stand at room temperature for another 2 days. Cyclohexane was removed using a rotary evaporator. The residue was diluted with acetone (50 mL), and the solution was poured into hexane (750 mL) to yield a white precipitate that was then collected by centrifugation (1000 rpm, 5 min). This reprecipitaiton cycle with acetone/hexane was repeated three times. The collected precipitate was then dissolved in ethanol (20 mL). The suspension was added under stirring to a mixture of 28% NH_3 aqueous solution (4.8 g) and ethanol (80 mL). After 1 h, a solution of BPE (0.5 g) and ethanol (5 mL) was added to the particle suspension, and the reaction was carried out for 20 h at ambient temperature. The reaction mixture was passed through a membrane filter (Millipore, Mitex, pore size 5 μm), and the filtrate was subjected to centrifugation (12 000 rpm, 20 min) to recover the surface-modified nanoparticles, which were subsequently washed three times by consecutive centrifugation and redispersion in ethanol.

Finally, the suspension of the ATRP initiator-fixed SiNPs was solvent-exchanged to *N*,*N*′-dimethylformamide (DMF) by repeated redispersion/centrifugation to obtain a DMF stock suspension. Yield: 0.81 g of solid.

ATRP-Initiator Fixation on SiNPs Prepared by the Lysine-Addition Technique. SiNP cores were prepared according to the method developed independently by Yokoi et al.[56] and Tsapatsis et al.[57,58] Typically, L-lysine (0.15 g) was dissolved in a solution of water (139 g) and octane (7.31 g) at 60 °C. Tetraethoxysilane (10.4 g) was added to the mixture, and the system was stirred for 20 h at 60 °C and then allowed to stand for 20 h at 100 °C. The reaction mixture was subjected to dialysis against water, using a regenerated cellulose tube (Spectrum Laboratories Ltd., Spectra/Por6, molecular cut off 8000), for 1 week to remove unreacted compounds. Ethylene glycol (35 g) was added to the dialyzed solution, and the mixture was subjected to rotary evaporation at 55 °C to remove water from the mixture. For the ATRP-initiator fixation, the residue containing SiNPs (2.6 g) was diluted with ethanol (20 mL), and a mixture of triethylamine (7.8 g) and ethanol (230 mL) and then a mixture of BPE (7.8 g) and ethanol (10 mL) were added to the particle solution, in that order. The reaction mixture was stirred for 2 days at room temperature. The system was concentrated in vacuo, and the residue was diluted with acetone (50 mL) and then added to hexane (800 mL) to obtain a white precipitate of the surface-modified nanoparticles. This reprecipitation cycle with an acetone/hexane system was repeated three times to purify the ATRP-initiator-fixed nanoparticles. Finally, the precipitate was dissolved in DMF, and the particle solution was concentrated in vacuo to remove volatile compounds, yielding a nanoparticle suspension in DMF to stock. Yield: 2.23 g of solid.

Surface-Initiated ATRP on SiNPs. Polymerization of MMA with the initiator-fixed SiNPs prepared by the reverse-micelle-mediated technique was carried out as follows: just before polymerization, the initiator-fixed SiNPs in DMF were solvent-exchanged to MMA to obtain a 1 wt % suspension in MMA. A Pyrex glass tube was charged with a predetermined amount of $Cu^{I}Cl$ (solid). A mixture of the initiator-fixed SiNP suspension in MMA containing a prescribed concentration of 2-(EiB)Br and dNbipy was quickly added to the Pyrex glass tube. The tube was equipped with a three-way stopcock, and the system was immediately degassed by three freeze−pump−thaw cycles and subsequently purged with argon. The mother reaction solution was divided nearly equally into a prescribed number of Pyrex glass tubes, each equipped with a three-way stopcock, in a glovebox purged with argon. The divided solution was degassed by one freeze−pump−thaw cycle and sealed off under vacuum. The polymerization was carried out in a shaking oil bath (TAITEC Corp., Saitama, Japan, Personal H-10) thermostated at 70 °C and, after a prescribed time *t*, quenched to room temperature. An aliquot of the solution was removed for NMR measurements to estimate monomer conversion, and for GPC measurements to determine the molecular weight and its distribution. The rest of the reaction mixture was diluted with acetone and centrifuged to collect the polymer-grafted SiNPs. The cycle of centrifugation and redispersion in acetone was repeated five times to obtain polymer-grafted SiNPs completely free of unbound (free) polymer. To determine the molecular weight of the graft polymer, PMMA chains were cleaved from the surface as follows: the polymer-grafted SiNPs (50 mg) and tetraoctylammonium bromide (50 mg), as a phase transfer catalyst, were dissolved in toluene (5 mL), to which a 10% HF aqueous solution (5 mL) was added. The mixture was vigorously stirred for 3 h. The cleaved polymer in the organic layer was subjected to GPC measurements.

In a typical run, the bulk polymerization of MMA was carried out at 70 °C for 4 h with the starting materials MMA (9.6 g, 96 mmol), 2-(EiB)Br (6.3 mg, 0.032 mmol), $Cu^{I}Cl$ (31 mg, 0.32 mmol), dNbipy (271 mg, 0.66 mmol), and initiator-fixed SiNPs of average diameter 55 nm (100 mg; the amount of initiator molecules fixed on the SiNP = 7.6 μmol). This gave a monomer conversion of 61%, a free polymer with M_n = 128 000 and M_w/M_n = 1.18, and a graft polymer with M_n = 122 000 and M_w/M_n = 1.19, where M_n and M_w are the number- and weight-average molecular weights, respectively, and M_w/M_n is the polydispersity index. The polymer-grafted SiNPs were purified by repeated cycles of centrifugation (12 000 rpm for 60 min) and redispersion in acetone (3 × 200 mL) and in THF (3 × 200 mL).

Polymerization of MMA with the initiator-fixed SiNPs prepared by the lysine-addition technique was carried out as follows. A Pyrex glass tube was charged with a predetermined amount of $Cu^{I}Cl$ (solid). A mixture of the initiator-fixed SiNP suspension in DMF, MMA, 2-(EiB)Br, and dNbipy was quickly added to the Pyrex glass tube. The polymerization and the characterization of the resultant polymers were carried out in a way similar to that used for the polymerization with SiNPs prepared by the reverse-micelle method, as described above.

In a typical run, the solution polymerization of MMA in DMF was carried out at 70 °C for 3 h with the starting materials MMA (8.9 g, 89 mmol), DMF (0.95 g), 2-(EiB)Br (28.8 mg, 0.148 mmol), $Cu^{I}Cl$ (14.6 mg, 0.15 mmol), dNbipy (121 mg, 0.30 mmol), and initiator-fixed SiNPs of average diameter 15 nm (50 mg; the amount of initiator molecules fixed on the SiNPs = 7.0 μmol), which gave a monomer conversion of 72% and a free polymer with M_n = 38 400 and M_w/M_n = 1.17, and a graft polymer with M_n = 35 300 and M_w/M_n = 1.15. The polymer-grafted SiNPs were purified by five cycles of centrifugation (20 000 rpm for 120 min) and redispersion in acetone (3 × 40 mL) and in THF (3 × 40 mL).

Results and Discussion

Synthesis of ATRP Initiator-Fixed SiNPs. The SiNP cores were prepared by the two methods: the reverse-micelle-mediated technique and the lysine-addition technique. The reverse-micelle-mediated technique provides highly monodisperse SiNPs with diameters of relative standard deviation around 5%. The particle size can be controlled by the composition of the reaction medium during preparation. We could tune the particle size to be within the range 30−70 nm by varying the Igepal CO-520 concentration. In this paper, we will focus on one sample, as a typical example, which has an average diameter of 55 nm as evaluated from its TEM image in Figure 1a. After formation of the SiNPs in the reverse micelles, we added a BPE solution to modify the particle surfaces with ATRP-initiating sites. To introduce a sufficient number of initiating sites, the modified SiNPs were further treated with BPE in ethanol in the presence of NH_3. In fact, without this additional step, the dispersibility of the nanoparticles in organic solvents was not good enough, and the subsequent surface grafting was unsatisfactory, yielding a low grafting density. To estimate the amount of initiator fixed on the SiNPs after the additional treatment, we carried out an elemental analysis and determined the bromine content to be 1.52%, which, along with the known density (1.9 g/cm^3) and the average diameter (55 nm) of the SiNPs, led to a surface density of about 2 initiator molecules/nm^2. The initiator-fixed SiNPs were highly dispersible in many organic solvents. A suspension in DMF formed no aggregates and could be stably stored in a refrigerator, without any change, for at least 1 year.

The synthesis of monodisperse SiNPs in the 10 nm range has until recently proven to be difficult. Yokoi et al. and Tsapatsis et al. independently introduced the formation of such particles via hydrolysis of tetraethoxysilane in aqueous lysine solution.[56−58] This method was adopted for the preparation of silica cores in the present work. Although the method can control the particle size in the range 5−20 nm, depending on the reaction conditions,[56−58] we used the reaction conditions described above for a typical example. Figure 1b shows a TEM image of the produced SiNPs. Although the shapes are not perfectly

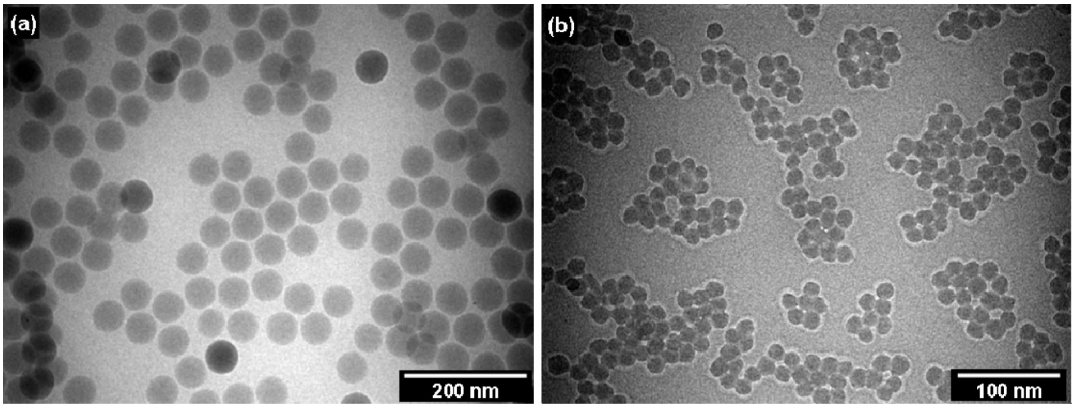

Figure 1. Transmission electron microscopic images of silica nanoparticles prepared by (a) the reverse-micelle-mediated technique and (b) the lysine-addition technique. The average diameters are (a) 55 nm and (b) 15 nm.

spherical, the size is nearly monodisperse, with an average diameter of 15 nm. BPE was used to decorate the surface of the resultant SiNPs with ATRP initiators. However, unlike the case for 55 nm SiNPs, described above, triethylamine was used as an alkaline catalyst instead of NH_3 because the addition of NH_3 induced aggregates of particles as soon as NH_3 was added to the system. Special care was also taken in the purification of the initiator-fixed SiNPs produced via the lysine-addition technique: if high-speed centrifugation is used to collect the SiNPs, they are difficult to redisperse homogeneously in solvents, even with the aid of ultrasonication. In practice, the initiator-fixed SiNPs were purified by reprecipitation with an acetone/hexane solvent system, and no aggregates were found after purification. Elemental analysis of the initiator-fixed SiNPs gave a bromine content of 5.60%, which led to a surface density of 2.4 initiator molecules/nm^2. This figure is comparable to those obtained for SiNPs prepared by the reverse-micelle-mediated technique described above, as well as with commercially available silica particles previously reported by us.[46] The dispersibility of initiator-fixed SiNPs with an average diameter of 15 nm in organic solvents is somewhat limited compared to other cases. For instance, the nanoparticles were perfectly dispersed in DMF, but not in toluene and anisole. This is the reason for using DMF as the stock solution.

Surface-Initiated ATRP of MMA from SiNPs. The initiator-fixed SiNPs were subsequently subjected to copper-mediated ATRP of MMA. According to our previous reports on SI-ATRP, the following two conditions are required to obtain a satisfactory result. First, the initiator-fixed SiNPs should never be dried before polymerization, to ensure their homogeneous dispersibility in the polymerization medium. Second, a "sacrificial" or free initiator, 2-(EiB)Br in this study, must be added to the polymerization mixture. The role of the free initiator is to accumulate an appropriate amount of Cu(II) species via the termination of polymer radicals at an early stage of polymerization and thus to control the polymerization by the so-called persistent radical effect.[59−61] Another role of the free initiator is to prevent interparticle coupling, causing gelation or particle aggregation, because free polymers produced by the free initiators will produce an entangled network structure through which the particle can hardly diffuse.

In the system with SiNPs prepared by the reverse-micelle-mediated technique, the suspension of the initiator-fixed SiNP in DMF was solvent-exchanged to the monomer to conduct bulk polymerization of MMA. Figure 2 shows the first-order kinetic plot of monomer concentration for the bulk polymerization of MMA with 2-(EiB)Br in the presence

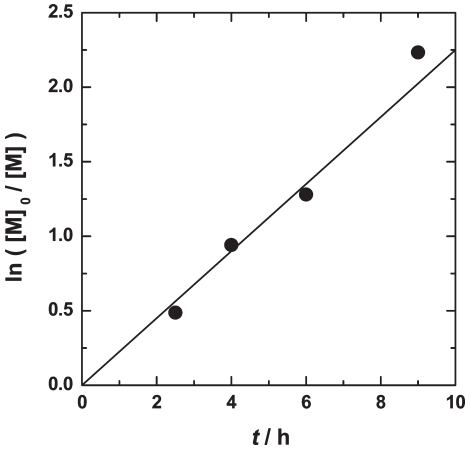

Figure 2. Plot of $\ln([M]_0/[M])$ vs t for the bulk polymerization of methyl methacrylate (MMA) at 70 °C with initiator-fixed silica nanoparticles of average diameter 55 nm (1 wt %): $[MMA]_0/[\text{ethyl 2-bromoisobutylate}]_0/[Cu^ICl]_0/[4,4'\text{-dinonyl-2,2'-bipyridine}]_0 = 3000/1/10/20$.

of BPE-functionalized SiNPs of average diameter 55 nm. The plot can be approximated by a straight line passing through the origin, thus giving first-order kinetics with respect to monomer conversion. The linear relationship reveals that the concentration of the propagating radical species is constant throughout the course of polymerization. SiNPs purified after polymerization were treated with HF to cleave the graft polymer from the surface, and the cleaved polymer was subjected to GPC analysis. Figure 3 shows the evolution of M_n and M_w/M_n of the cleaved graft polymer and of the free polymer simultaneously produced from the free initiator 2-(EiB)Br. The dotted line shows the theoretical value of M_n ($M_{n,theo} = M_{MMA} \times C \times [MMA]_0/([2\text{-(EiB)Br}]_0 + [\text{initiation sites available on SiNP surface}]_0)$), where M_{MMA} is the molecular weight of MMA, C is the conversion, and $[MMA]_0$ and $[2\text{-(EiB)Br}]_0$ are the concentrations of MMA and 2-(EiB)Br in the feed, respectively. The initiation sites available on the SiNP surfaces were estimated from the polymer grafting density, as will be described below. It can be seen that the M_n values of the graft and free polymers are nearly the same, both increasing in proportion to monomer conversion. These M_n values agree well with $M_{n,theo}$. The M_w/M_n ratio remains fairly low, around 1.2 for most samples. All these results confirm that the polymerization of MMA initiated from the SiNP surfaces proceeds in a living fashion, giving SiNPs with well-defined PMMA (PMMA-SiNP).

For the polymerization with the SiNPs prepared by the lysine-addition technique, a suspension of the BPE-functionalized

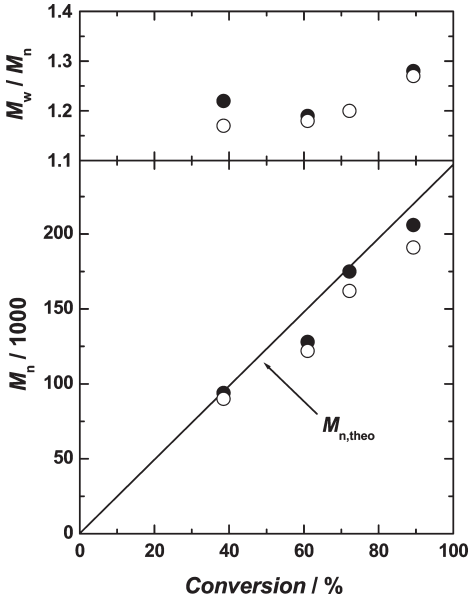

Figure 3. Evolution of number-average molecular weight (M_n) and polydispersity index (M_w/M_n) of the graft (○) and free (●) polymers as a function of monomer conversion for the bulk polymerization of methyl methacrylate (MMA) at 70 °C with initiator-fixed silica nanoparticles of average diameter 55 nm (1 wt %): $[MMA]_0/[ethyl\ 2\text{-}bromoisobutylate]_0/[Cu^ICl]_0/[4,4'\text{-}dinonyl\text{-}2,2'\text{-}bipyridine]_0 = 3000/1/10/20$.

SiNPs in DMF was used directly to prepare a solution for polymerization because the SiNPs, once centrifuged at high-speed rotation, were not redispersed homogeneously in solution. Solution polymerization of MMA in DMF (10 wt %) was carried out with the initiator-fixed nanoparticles in the presence of 2-(EiB)Br. Similar to the polymerization with the 55 nm SiNPs mentioned above, the polymerization proceeded in a living manner, showing a linear relationship for $\ln[M]_0/[M]$ vs t, as shown in Figure 4, and a proportional increase in M_n of the produced polymers as a function of monomer conversion, and relatively low M_w/M_n values, as shown in Figure 5.

Polymer Grafting Density. Thermogravimetric analyses of the PMMA-SiNP hybrids were carried out to estimate the mass (w) of polymer grafted on the SiNPs. The graft density (σ) was then calculated using eq 1:

$$\sigma = (w/M_n)A_v/(\pi d_c^2) \quad (1)$$

where d_c is the diameter of the SiNP core and A_v is Avogadro's number. For the PMMA-SiNPs with a core diameter of 55 nm (see Figures 2 and 3 for the polymerization data for the SiNP core), the graft density is nearly constant, independent of the polymerization time, and approximately equal to 0.8 chains/nm^2, as shown in Figure 6a. In the case of polymerization with SiNP cores of 15 nm (see Figures 4 and 5 for the polymerization data), as can be seen in Figure 6b, the graft density ranges from 0.4 to 0.5 chains/nm^2, which is somewhat smaller than in the case of polymerization with 55 nm SiNP cores. The reason for this is not at present clear, but it may possibly be due to some experimental error in determining the core diameters. More importantly, the graft densities obtained are high enough to demonstrate that the layer of polymer grafts is in the concentrated-brush regime.

DLS Measurements of PMMA-SiNPs. The PMMA-SiNPs obtained here are well dispersed in most common solvents for PMMA. DLS measurements were conducted for a series of hybrid particles in dilute acetone solution. Parts a and b of Figure 7 show the hydrodynamic diameters D_h for

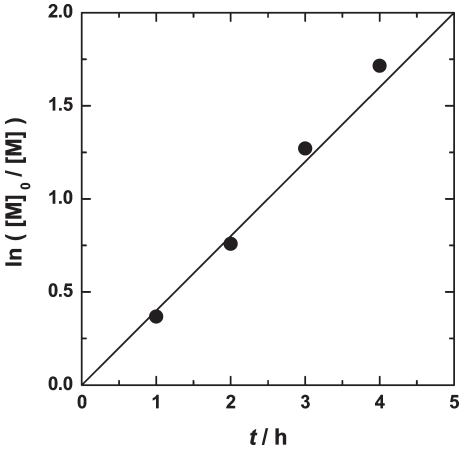

Figure 4. Plot of $\ln([M]_0/[M])$ vs t for solution polymerization of methyl methacrylate (MMA) in N,N-dimethylformamide (10 wt %) at 70 °C with initiator-fixed silica nanoparticles of average diameter 15 nm (0.5 wt %): $[MMA]_0/[ethyl\ 2\text{-}bromoisobutylate]_0/[Cu^ICl]_0/[4,4'\text{-}dinonyl\text{-}2,2'\text{-}bipyridine]_0 = 600/1/2/4$.

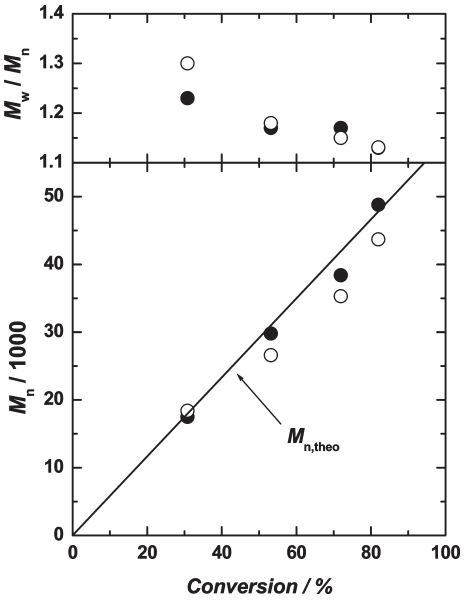

Figure 5. Evolution of number-average molecular weight (M_n) and polydispersity index (M_w/M_n) of the graft (○) and free (●) polymers as a function of monomer conversion for solution polymerization of methyl methacrylate (MMA) in N,N-dimethylformamide (10 wt %) at 70 °C with initiator-fixed silica nanoparticles of average diameter 15 nm (0.5 wt %): $[MMA]_0/[ethyl\ 2\text{-}bromoisobutylate]_0/[Cu^ICl]_0/[4,4'\text{-}dinonyl\text{-}2,2'\text{-}bipyridine]_0 = 600/1/2/4$.

the hybrid particles with the core diameters of 55 and 15 nm, respectively, as a function of the M_w of the PMMA grafts. The diameters of the compact core−shell model[33] and the fully stretched core−shell model[33] are also shown in the figures. The former model consists of a SiNP core and a PMMA shell of bulk density, and the latter consists of a SiNP core and a PMMA shell whose size is equal to that of the PMMA chains radially stretched in an all-trans conformation. In both cases, the D_h value increases with increasing M_w, being intermediate between the diameters of the two models.

Formation of Two Dimensional Ordered Arrays. PMMA-SiNPs monolayers were prepared following a previously reported procedure.[46,49] Briefly, a droplet of a concentrated suspension of PMMA-SiNPs in toluene was deposited

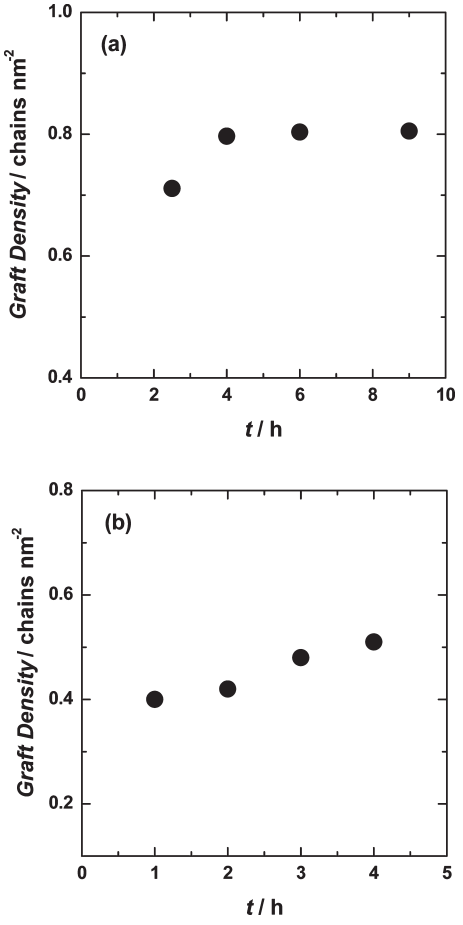

Figure 6. Time dependence of the graft density of poly(methyl methacrylate) grown from the surfaces of silica nanoparticles of average diameter (a) 55 nm and (b) 15 nm.

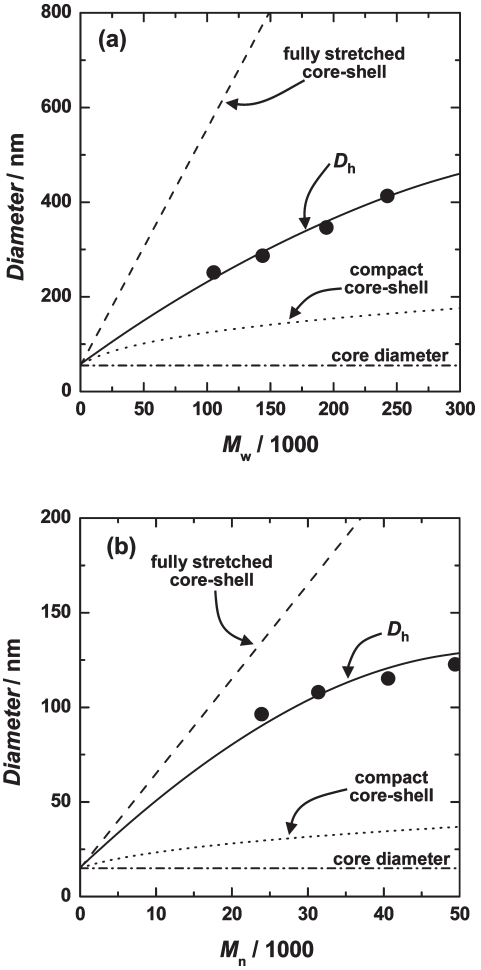

Figure 7. Plot of average hydrodynamic diameter D_h of silica nanoparticles grafted with poly(methyl methacrylate) (PMMA-SiNP) as a function of weight-average molecular weight M_w of the PMMA graft chains. The D_h values were determined by dynamic light scattering in dilute acetone suspension at 30 °C. The diameters of the SiNP cores are (a) 55 nm and (b) 15 nm. The broken and dotted lines represent the diameters of the fully stretched and compact core−shell models, respectively (see text).[33].

onto the surface of purified water, giving a thin film at the air−water interface as the toluene evaporated. This thin film was transferred onto a TEM grid. Figure 8 shows the TEM images of transferred monolayers for PMMA-SiNPs with a core diameter of 55 nm and different molecular weights of PMMA grafts (M_n = (a) 90 000, (b) 191 000), and transferred monolayers with core diameters of 15 nm and different molecular weights of PMMA grafts (M_n = (c) 17 500, (d) 43 700). In all cases, the SiNP cores, visible as dark circles, are uniformly dispersed throughout the film; while the PMMA chains, which should form fringes surrounding the SiNP cores, are hardly seen because of their much lower electron density. The center-to-center distance between the nearest-neighbor particles increased with increasing molecular weight of graft chains. Interestingly, the hybrid particles with 55 nm cores are hexagonally close-packed in a monolayer. This is in contrast to the case for the hybrids of 15 nm SiNP cores, which do not form an ordered array, probably due to somewhat higher polydispersity in size and shape.

Formation of Colloidal Crystals. We previously identified a colloidal crystal in a suspension of hybrid particles having a spherical silica core and a shell of well-defined PMMA concentrated brush.[50−52] Following the same procedure, fabrication of a colloidal crystal was attempted using the PMMA-SiNPs prepared in the present work. Briefly, the PMMA-SiNP hybrid particles used here have a SiNP core of average diameter 55 nm and a shell of PMMA graft chains of M_n = 122 000 and M_w/M_n = 1.19, end-grafted on the SiNP surface with a surface density as high as 0.8 chains/nm^2. The hybrid particles were suspended in a mixture of chlorobenzene/1,2-dichloroethane of volume composition 66/34. The 6.14 vol % particle suspension was allowed to stand at ambient temperature. Tiny iridescent flecks were observed several minutes after the onset of the experiment, indicating the formation of Bragg-reflecting crystallites, and the formed crystallites filled the whole volume of the suspension, as shown in Figure 9.

The PMMA-SiNP suspension was subjected to confocal laser scanning microscopic (CLSM) measurement to examine the crystal structure visually. Figure 10 shows a CLSM image of a two-dimensional slice inside the sample. The SiNP cores of the hybrid particles are clearly visible as yellow dots forming a two-dimensional hexagonal array, while the PMMA brush layers are hardly visible because of their much lower reflectivity. The mean nearest-neighbor center-to-center distance D_{dis} between particles was found to be 350 nm (Figure 10). The distance can be estimated from the particle volume fraction ϕ in the crystal, according to the following relation, which is valid for closed-packed structures:[51,52]

$$D_{dis,cal} = 2^{1/6}(V_p/\phi)^{1/3} \quad (2)$$

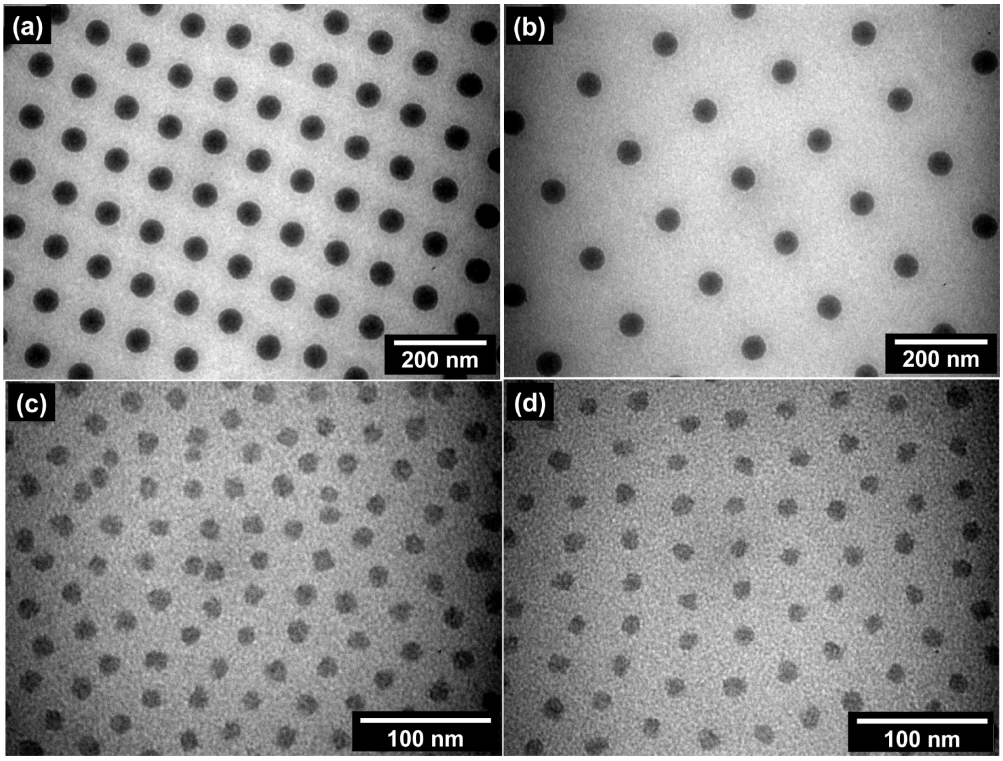

Figure 8. Transmission electron microscopic images of the transferred films of silica nanoparticles end-grafted with poly(methyl methacrylate) brushes (PMMA-SiNPs): the average diameters of the silica particle cores are (a, b) 55 and (c, d) 15 nm. Number-average molecular weights of the graft polymers are (a) 90 000, (b) 191 000, (c) 17 500, and (d) 43 700.

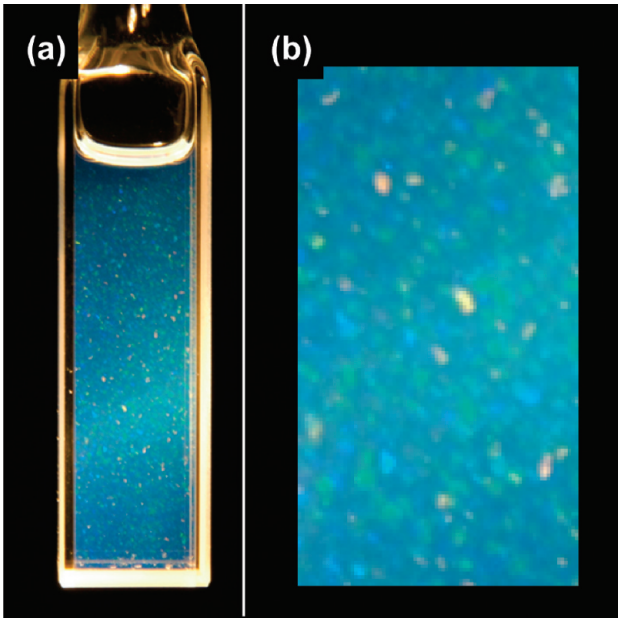

Figure 9. Photographs of a suspension of silica nanoparticles end-grafted with poly(methyl methacrylate) brushes (PMMA-SiNP) in a mixed solvent (chlorobenzene/1,2-dichloroethane, 66/34 volume ratio) illuminated from behind by white light. The number-average molecular weight of the PMMA graft is 122 000 and the average diameter of the SiNP core is 55 nm. The weight fraction of PMMA-SiNP was 6.14 vol %. (b) is a close-up of (a).

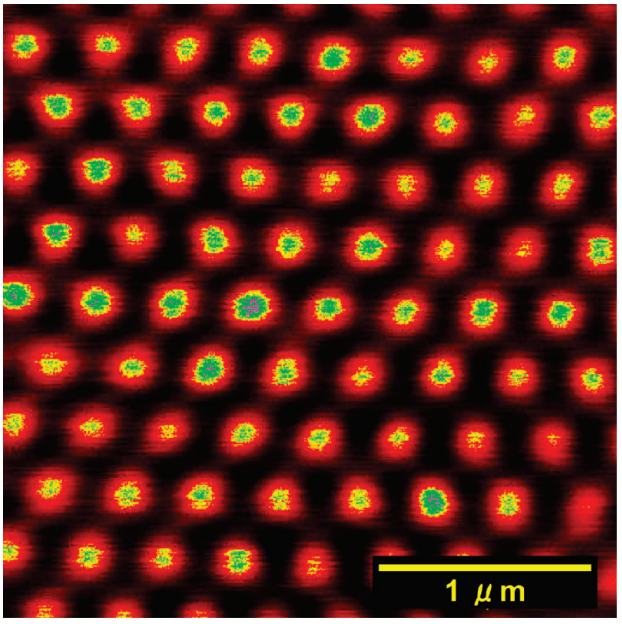

Figure 10. Confocal laser scanning microscopic image of colloidal crystals of silica nanoparticles end-grafted with poly(methyl methacrylate) brushes (PMMA-SiNP). Observations were performed using an Ar laser of wavelength 488 nm and ×63 objective in reflection mode. The distance of the focal plane from the inside of the coverslip was 50 μm. The diameter of the SiNP cores is 55 nm. The number-average molecular weight of the PMMA graft is 122 000. The mean nearest-neighbor interparticle distance is 350 nm.

where V_p is the volume of a PMMA-SiNP particle in units of nm^3. The $D_{dis,cal}$ value was calculated to be 320 nm, which is in good agreement with the experimentally observed D_{dis} value and has a good correlation with the hydrodynamic diameter D_h = 290 nm of the hybrid particle determined in dilute suspension. This confirms the uniformity of the crystal as well as the consistency of the relevant experimental procedures.

Conclusions

It was demonstrated that narrowly size-distributed SiNPs with average diameters less than 100 nm could be surface-decorated with ATRP initiation sites, while retaining their high dispersibility in solution. Surface-initiated ATRP of MMA using these functionalized SiNPs proceeded in a living fashion, yielding structurally controlled hybrid nanoparticles with a SiNP core and a shell of variable thickness composed of well-defined, concentrated PMMA brushes. Thanks to their exceptionally good dispersibility in solvents, these hybrid particles formed two- or three-dimensional ordered arrays with a high degree of structural order and wide controllability of the interparticle distances.

Acknowledgment. This work was supported in part by a Grant-in-Aid for Scientific Research (Grant-in-Aid 17685010) from the Ministry of Education, Culture, Sports, Science, and Technology, Japan, and by the Industrial Technology Research Grant Program in 2004 and 2009 from the New Energy and Industrial Technology Development Organization (NEDO) of Japan. We thank Chisso Corporation for their kind donation of tetraethoxysilane and triethoxysilane.

References and Notes

(1) Tsujii, T.; Ohno, K.; Yamamoto, S.; Goto, A.; Fukuda, T. *Adv. Polym. Sci.* **2006**, *197*, 1–45.
(2) Radhakrishnan, B.; Ranjan, R.; Brittain, W. J. *Soft Matter* **2006**, *2*, 386–396.
(3) Edmonson, S.; Osborne, V. L.; Huck, W. T. S. *Chem. Soc. Rev.* **2004**, *33*, 14–22.
(4) Barbey, R.; Lavanant, L.; Paripovic, D.; Schüwer, N.; Sugnaux, C.; Tugulu, S.; Klok, H.-A. *Chem. Rev.* **2009**, *109*, 5437–5527.
(5) Matyjaszewski, K.; Xia, J. *Chem. Rev.* **2001**, *101*, 2921–2990.
(6) Kamigaito, M.; Ando, T.; Sawamoto, M. *Chem. Rev.* **2001**, *101*, 3689–3745.
(7) Hawker, C. J.; Bosman, A. W.; Hart, E. *Chem. Rev.* **2001**, *101*, 3661–3688.
(8) Perrier, S.; Tackolpuckdee, P. *J. Polym. Sci., Part A Polym. Chem.* **2005**, *43*, 5347–5393.
(9) Goto, A.; Fukuda, T. *Prog. Polym. Sci.* **2004**, *29*, 329–385.
(10) Fukuda, T.; Goto, A.; Ohno, K. *Macromol. Rapid Commun.* **2000**, *21*, 151–165.
(11) von Werne, T.; Patten, T. E. *J. Am. Chem. Soc.* **1999**, *121*, 7409–7410.
(12) von Werne, T.; Patten, T. E. *J. Am. Chem. Soc.* **2001**, *123*, 7497–7505.
(13) Pyun, J.; Matyjaszewski, K.; Kowalewski, T.; Savin, D.; Patterson, G.; Kickelbick, G.; Huesing, N. *J. Am. Chem. Soc.* **2001**, *123*, 9445–9446.
(14) Pyun, J.; Jia, S. J.; Kowalewski, T.; Patterson, G. D.; Matyjaszewski, K. *Macromolecules* **2003**, *36*, 5094–5104.
(15) Carrot, G.; Diamanti, S.; Manuszak, M.; Charleux, B.; Vairon, I. P. *J. Polym. Sci., Part A: Polym. Chem.* **2001**, *39*, 4294–4301.
(16) Mori, H.; Seng, D. C.; Zhang, M. F.; Muller, A. H. E. *Langmuir* **2002**, *18*, 3682–3693.
(17) Chen, X. Y.; Armes, S. P. *Adv. Mater.* (*Weinheim, Ger.*) **2003**, *15*, 1558–1562.
(18) Chen, X. Y.; Armes, S. P.; Greaves, S. J.; Watts, J. F. *Langmuir* **2004**, *20*, 587–595.
(19) El Harrak, A.; Carrot, G.; Oberdisse, J.; Eychenne-Baron, C.; Boue, F. *Macromolecules* **2004**, *37*, 6376–6384.
(20) Perruchot, C.; Khan, M. A.; Kamitsi, A.; Armes, S. P. *Langmuir* **2001**, *17*, 4479–4481.
(21) Schepelina, O.; Zharov, I. *Langmuir* **2006**, *22*, 10523–10527.
(22) Husseman, M.; Malmström, E. E.; McNamara, M.; Mate, M.; Mecerreyes, D.; Benoit, D. G.; Hedrick, J. L.; Mansky, P.; Huang, E.; Russel, T. P.; Hawker, C. J. *Macromolecules* **1999**, *32*, 1424–1431.
(23) Kasseh, A.; Ait-kadi, A.; Riedl, B.; Pierson, J. F. *Polymer* **2003**, *44*, 1367–1375.
(24) Bartholome, C.; Beyou, E.; Bourgeat-Lami, E.; Chaumont, P.; Zydowicz, N. *Macromolecules* **2003**, *36*, 7946–7952.
(25) Bartholome, C.; Beyou, E.; Bourgeat-Lami, E.; Chaumont, P.; Zydowicz, N. *Polymer* **2005**, *46*, 8502–8510.
(26) Bartholome, C.; Beyou, E.; Bourgeat-Lami, E.; Chaumont, P.; Lefebvre, F.; Zydowicz, N. *Macromolecules* **2005**, *38*, 1099–1106.
(27) Parvolle, J.; Montfort, J. P.; Billon, L. *Macromol. Chem. Phys.* **2004**, *205*, 1369–1378.
(28) Parvolle, J.; Laruelle, G.; Khoukh, A.; Billon, L. *Macromol. Chem. Phys.* **2005**, *206*, 372–382.
(29) Ghannam, L.; Parvole, J.; Laruelle, G.; Francois, J.; Billon, L. *Polym. Int.* **2006**, *55*, 1199–1207.
(30) Nuss, S.; Böttcher, H.; Wurm, H.; Hallensleben, M. L. *Angew. Chem., Int. Ed.* **2001**, *40*, 4016–4018.
(31) Mandal, T. K.; Fleming, M. S.; Walt, D. R. *Nano Lett.* **2002**, *2*, 3–7.
(32) Ohno, K.; Koh, K.; Tsujii, Y.; Fukuda, T. *Macromolecules* **2002**, *35*, 8989–8993.
(33) Ohno, K.; Koh, K.; Tsujii, Y.; Fukuda, T. *Angew. Chem., Int. Ed.* **2003**, *42*, 2751–2754.
(34) Wang, Y.; Teng, X. W.; Wang, J. S.; Yang, H. *Nano Lett.* **2003**, *3*, 789–793.
(35) Marutani, E.; Yamamoto, S.; Ninjbadgar, T.; Tsujii, Y.; Fukuda, T.; Takano, M. *Polymer* **2004**, *45*, 2231–2235.
(36) Gelbrich, T.; Feyen, M.; Schmidt, A. M. *Macromolecules* **2006**, *39*, 3469–3472.
(37) Lattuada, M.; Hatton, T. A. *Langmuir* **2007**, *23*, 2158–2168.
(38) Sun, Y.; Ding, X.; Zheng, Z.; Cheng, X.; Hu, X. *Eur. Polym. J.* **2007**, *43*, 762–772.
(39) Vestal, C. R.; Zhang, Z. J. *J. Am. Chem. Soc.* **2002**, *124*, 14312–14313.
(40) Matsuno, R.; Otsuka, H.; Takahara, A. *Soft Matter* **2006**, *2*, 415–421.
(41) Zheng, G. D.; Stover, H. D. H. *Macromolecules* **2002**, *35*, 7612–7619.
(42) Jayachandran, K. N.; Takacs-Cox, A.; Brooks, D. E. *Macromolecules* **2002**, *35*, 4247–4257.
(43) Kizhakkedathu, J. N.; Norris-Jones, R.; Brooks, D. E. *Macromolecules* **2004**, *37*, 734–743.
(44) Liu, T. Q.; Jia, S.; Kowalewski, T.; Matyjaszewski, K.; Casado-Portilla, R.; Belmont, J. *Langmuir* **2003**, *19*, 6342–6345.
(45) Homenick, C. M.; Lawson, G.; Adronov, A. *Polym. Rev.* **2007**, *47*, 265–290.
(46) Ohno, K.; Morinaga, T.; Koh, K.; Tsujii, Y.; Fukuda, T. *Macromolecules* **2005**, *38*, 2137–2142.
(47) Morinaga, T.; Ohkura, M.; Ohno, K.; Tsujii, Y.; Fukuda, T. *Macromolecules* **2007**, *40*, 1159–1164.
(48) Ladmiral, V.; Morinaga, T.; Ohno, K.; Fukuda, T.; Tsujii, Y. *Eur. Polym. J.* **2009**, *45*, 2788–2796.
(49) Morinaga, T.; Ohno, K.; Tsujii, Y.; Fukuda, T. *Eur. Polym. J.* **2007**, *43*, 243–248.
(50) Ohno, K.; Morinaga, T.; Takeno, S.; Tsujii, Y.; Fukuda, T. *Macromolecules* **2006**, *39*, 1245–1249.
(51) Ohno, K.; Morinaga, T.; Takeno, S.; Tsujii, Y.; Fukuda, T. *Macromolecules* **2007**, *40*, 9143–9150.
(52) Morinaga, T.; Ohno, K.; Tsujii, Y.; Fukuda, T. *Macromolecules* **2008**, *41*, 3620–3626.
(53) Stöber, W.; Fink, A.; Bohn, A. *J. Colloid Interface Sci.* **1968**, *26*, 62–69.
(54) Osseo-Asare, K.; Arriagada, F. J. *Colloids Surf.* **1990**, *50*, 321–329.
(55) Osseo-Asare, K.; Arriagada, F. J. *J. Colloid Interface Sci.* **1990**, *50*, 321–329.
(56) Yokoi, T.; Sakamoto, Y.; Terasaki, O.; Kubota, Y.; Okuto, T.; Tatsumi, T. *J. Am. Chem. Soc.* **2006**, *128*, 13664–13665.
(57) Davis, T. M.; Snyder, M. A.; Krohn, J. E.; Tsapatsis, M. *Chem. Mater.* **2006**, *18*, 5814–5816.
(58) Snyder, M. A.; Alex Lee, J.; Davis, T. M.; Scriven, L. E.; Tsapatsis, M. *Langmuir* **2007**, *23*, 9924–9928.
(59) Ejaz, M.; Yamamoto, S.; Ohno, K.; Tsujii, Y.; Fukuda, T. *Macromolecules* **1998**, *31*, 5934–5936.
(60) Ejaz, M.; Ohno, K.; Tsujii, Y.; Fukuda, T. *Macromolecules* **2000**, *33*, 2870–2874.
(61) Fischer, H. *Chem. Rev.* **2001**, *101*, 3581–3610.